

*Original scientific paper*

## **CORROSION RESISTANCE of X12CrMoWVNbN10-1-1 STEEL in NaCl SOLUTIONS at DIFFERENT pH VALUES**

**Jovanka Pejić<sup>1</sup>, Borut Kosec<sup>2</sup>, Olga Pantić<sup>1</sup>, Tatjana Volkov Husović<sup>3</sup>, Matija Zorc<sup>2</sup>, Milica Vlahović<sup>1</sup>**

**Received:** January 11, 2025

**Accepted:** January 29, 2025

**Abstract:** The influence of pH on the corrosion behavior of X12CrMoWVNbN10-1-1 steel was examined in 0.1 M NaCl solution. The rate of general (uniform) corrosion of the tested steel was determined using linear polarization resistance (LPR) and electrochemical impedance spectroscopy (EIS) methods. In the NaCl solution with a pH of 2.9, the tested steel exhibited a more negative corrosion potential and lower corrosion resistance. Significantly higher corrosion potential and resistance to general corrosion were observed in a neutral solution (pH = 6.5), where the steel was in a passive state.

**Keywords:** Alloy steels, Corrosion, Passive layer, Electrochemical methods

### **1 INTRODUCTION**

X12CrMoWVNbN10-1-1 steel is a high-alloy ferritic-martensitic steel used primarily in thermal power plants, especially in steam generators, due to its exceptional properties. This steel exhibits resistance to plastic deformation at high temperatures, good toughness, and resistance to radiation and corrosion in elevated temperature environments. These properties make X12CrMoWVNbN10-1-1 steel well-suited for applications in industries that demand high-temperature performance and exceptional mechanical characteristics (Bendick and Ring, 1996; Haarmann et al., 2002; Little, 1972; Garr, Rhodes and Kramer, 1973).

<sup>1</sup> University of Belgrade, Institute of Chemistry, Technology and Metallurgy- National Institute of the Republic of Serbia, Njegoševa 12, Belgrade, Serbia

<sup>2</sup> University of Ljubljana, Faculty of Natural Sciences and Engineering, Aškerčeva cesta 12, Ljubljana, Slovenia

<sup>3</sup> University of Belgrade, Faculty of Technology and Metallurgy, Karnegijeva 4, Belgrade, Serbia

E-mails: [jovanka.kovacina@ihtm.bg.ac.rs](mailto:jovanka.kovacina@ihtm.bg.ac.rs), ORCID: 0000-0002-3494-9180; [borut.kosec@ntf.uni-lj.si](mailto:borut.kosec@ntf.uni-lj.si), ORCID: 0009-0001-8117-9721; [olga.pantic@ihtm.bg.ac.rs](mailto:olga.pantic@ihtm.bg.ac.rs), ORCID: 0000-0003-4667-2585; [tatjana@tmf.bg.ac.rs](mailto:tatjana@tmf.bg.ac.rs), ORCID: 0000-0002-2667-5802; [matija.zorc@ntf.uni-lj.si](mailto:matija.zorc@ntf.uni-lj.si), ORCID: 0009-0002-8792-0549; [m.vlahovic@ihtm.bg.ac.rs](mailto:m.vlahovic@ihtm.bg.ac.rs), ORCID: 0000-0002-7893-9101

Since X12CrMoWVNbN10-1-1 steel is used under extreme conditions, its high corrosion resistance is crucial. This includes resistance to corrosion in the presence of the vapor phase and various types of electrolytes, particularly those with an acidic nature. The most common form of corrosion in acidic electrolytes is general (or uniform) corrosion, which involves the uniform dissolution of the metal surface, leading to a gradual reduction in the steel's thickness.

A quantitative indicator of general (uniform) corrosion is the corrosion rate, which can be determined in different ways.

Electrochemical techniques allow for the determination of parameters such as polarization resistance ( $R_p$ ) and corrosion current density ( $j_{\text{corr}}$ ). The corrosion rate ( $v_{\text{corr}}$ ) can be directly calculated from the corrosion current density using Faraday's law. Additionally, polarization resistance is related to corrosion current density through a corresponding equation.

In this study, the general (uniform) corrosion rate of X12CrMoWVNbN10-1-1 steel in acidic and neutral NaCl solutions was determined using two electrochemical methods—linear polarisation resistance (LPR) and electrochemical impedance spectroscopy (EIS). The values of polarization resistance ( $R_p$ ) and corrosion current density ( $j_{\text{corr}}$ ) were used as indicators of resistance to general corrosion.

## 2 EXPERIMENTAL

### 2.1 Material characterization

The standard chemical composition of the tested steel (Materials Number 1.4906, X12CrMoWVNbN10-1-1) (ASTM A335, 2022), as well as the values determined by the XRF method using an Olympus Vanta C Series Handheld XRF Analyzer, are presented in Table 1.

**Table 1** Chemical composition of the X12CrMoWVNbN10-1-1 steel (wt. %)

	C	Si	Mn	Cr	Mo	Ni	V	W	Nb	N	S
Standard	0.10		0.40		1.00	0.60	0.15	0.95		0.04	
	-	≤	-	10.0 -	-	-	-	-	0.04 -	-	≤
		0.12		11.0					0.06		0.007
	0.14		0.60		1.20	0.80	0.25	1.10		0.07	
XRF	-	0.92	0.49	10.16	1.05	0.77	0.17	0.92	0.055		0.11

The tested steel contains a high concentration of chromium (Table 1), which allows it to exhibit stainless steel-like behavior under approximately neutral conditions. Before the

electrochemical tests, the X12CrMoWVNbN10-1-1 steel samples were ground with abrasive paper up to 1500 grit, degreased with ethanol, rinsed with distilled water, and air-dried. The samples were then stored in a desiccator until the start of the tests

## 2.2 Electrochemical testing

Two 0.1 M NaCl solutions, prepared with bidistilled water, were used for electrochemical tests. The first solution had a pH of 2.9 (acidic solution), adjusted by carefully adding 0.1 M HCl, while the second solution had a pH of 6.5 (neutral solution). The pH value was measured using a HANNA Instruments HI 2210 device.

### Linear Polarisation resistance (LPR) method

LPR measurements were performed at room temperature in both acidic and neutral chloride-containing solutions. The tests were conducted in a standard three-electrode electrochemical cell using a potentiostat/galvanostat/ZRA GAMRY 620. The working electrode was the steel specimen (with a working area of 1 cm<sup>2</sup>), the reference electrode was a Saturated Calomel Electrode (SCE), and the auxiliary electrode was a Pt-mesh. After achieving a stable corrosion potential ( $E_{\text{corr}}$ ), the specimens were polarized within a narrow potential range ( $E = \pm 10$  mV) relative to  $E_{\text{corr}}$ , starting from the cathodic to the anodic region, and the corresponding current density ( $j$ ) was recorded. The potential sweep rate was 0.166 mVs<sup>-1</sup>. The polarization resistance ( $R_p$ ) was determined as the slope of the recorded E-j curve at the  $E_{\text{corr}}$ .

### Electrochemical Impedance spectroscopy (EIS) method

EIS measurements were carried out in both acidic and neutral chloride-containing solutions. After stabilizing the corrosion potential ( $E_{\text{corr}}$ ), a sinusoidal potential of amplitude  $\pm 10$  mV vs.  $E_{\text{corr}}$  across a frequency range from 100,000 Hz to 0.001 Hz was applied to the specimen (with a working area of 1 cm<sup>2</sup>). The reference electrode was SCE, and the auxiliary electrode was Pt-mesh. Measurements were conducted using the potentiostat/galvanostat/ZRA GAMRY 620, and the EIS data were analyzed and fitted using the Gamry Echem Analyst software.

## 2.3 Optical microscopy

The surface morphology of the tested specimens, both before and after electrochemical testing, was analyzed using a Delta Optical Smart 5MP PRO digital USB microscope, accompanied by the Delta Optical Smart Analysis Pro software package.

### 3 RESULTS AND DISCUSSION

#### 3.1 LPR measurements

Polarisation (potential-current density, E-j) diagrams obtained using the LPR technique in solutions with different pH values are shown in Figure 1

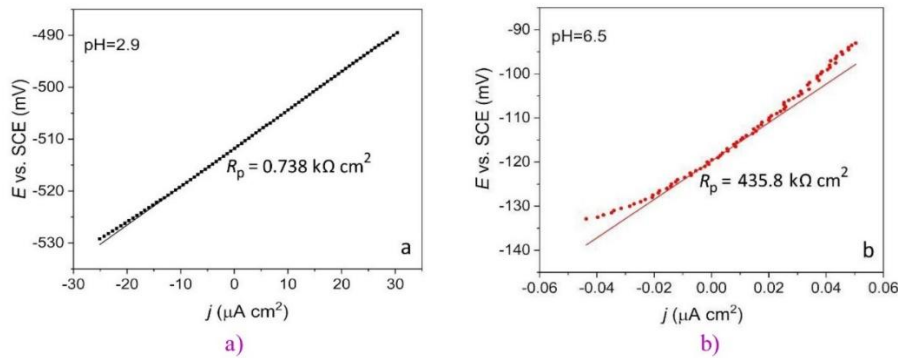


**Figure 1** LPR diagrams in: a) acidic (pH=2.9) solution, b) neutral (pH=6.5) solution

The slope of the curve ( $\Delta E/\Delta j$ ) at the corrosion potential ( $E_{\text{corr}}$ ) corresponds to the polarization resistance ( $R_p$ ) value. The  $R_p$  value in the acidic solution is significantly lower than in the neutral solution.

#### 3.2 EIS measurements

Nyquist plots obtained in solutions with different pH values are shown in Figure 2a), with an enlarged view of the initial portion in Figure 2b).

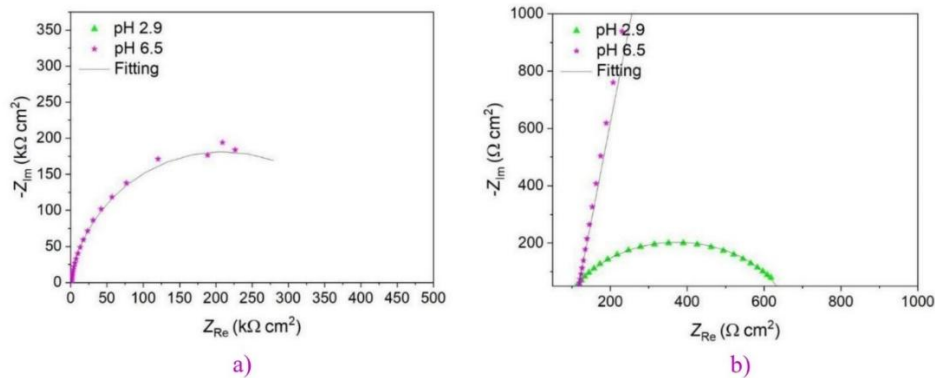


**Figure 2** EIS diagrams for: a) Nyquist plot for the tested steel, b) Enlarged view of the Nyquist plot for the tested steel

The Nyquist plot (Figure 2a) displays the relationship between the real impedance component ( $Z_{Re}$ ) and the imaginary impedance component ( $-Z_{Im}$ ) in linear coordinates. The diameter of the semicircle corresponds to the polarization resistance ( $R_p$ ) value. A larger diameter indicates a higher  $R_p$  value, and thus higher corrosion resistance.

The  $R_p$  values in acidic and neutral NaCl solutions are approximately  $0.560 \text{ k}\Omega \text{ cm}^2$  and  $420 \text{ k}\Omega \text{ cm}^2$ , respectively. As expected, the tested steel demonstrates the lowest resistance to general corrosion in the acidic environment. This can be attributed to the high concentration of hydrogen ions in the acidic solution, which accelerates corrosion and leads to intense dissolution of the steel.

In the neutral solution, two-time constants are observed. One corresponds to electrochemical processes occurring in the passive layer, while the other corresponds to processes at the metal/passive layer interface. Since these time constants are associated with frequencies at the lower end of the spectrum, the experimental EIS results were fitted using a simplified Equivalent Electrical Circuit (EEC) (Figure 3), with a single time constant.

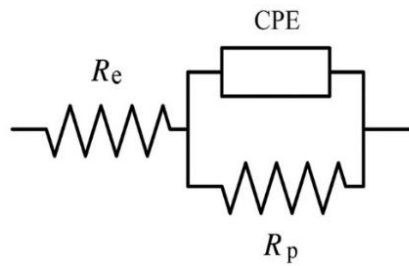


**Figure 3** Equivalent electrical circuit (EEC) used for fitting EIS results ( $R_p$  - polarization resistance,  $R_e$  - electrolyte resistance, CPE- constant phase element)

In the EEC, the CPE replaces the double-layer capacitance ( $C_{dl}$ ) at the surface of the tested steel. The CPE accounts for the microstructural inhomogeneities of the steel surface, such as surface roughness and segregation of alloying elements (Srinivasan and Fasmin, 2021). The effective capacitance of the passive film ( $C_{eff}$ ) was determined using the Brug equation (Eq. 1) with the corresponding values for  $R_p$ ,  $Q$ , and  $n$  (Hirschorn et al., 2010)

$$C_{eff} = R_p^{\frac{1-n}{n}} \cdot Q^{\frac{1}{n}} \quad (1)$$

The results obtained are presented in Table 2.

**Table 2** Results of EIS measurements in acid and neutral solutions for the tested steel

pH	$R_p$ ( $k\Omega\text{ cm}^2$ )	CPE		$C_{\text{eff}}$ ( $\mu\text{F cm}^{-2}$ )
		$Y_0/10^{-6}$ ( $\text{s } \Omega^{-1}\text{ cm}^{-2}$ )	n	
2.9	0.557	260.0	0.800	901.9
6.5	418.5	37.15	0.910	96.50

### 3.3 Summary of General (Uniform) Corrosion Measurements

Table 3 summarizes the results of electrochemical tests conducted using the LPR and EIS methods.

**Table 3** Summary results ( $R_p$ ) of electrochemical methods for the tested steel

pH	$R_p$ ( $k\Omega\text{ cm}^2$ )	
	LPR	EIS
2.9	0.738	0.557
6.5	435.8	418.5

The results from both the LPR and EIS methods indicate that the general corrosion rate, as expressed by the value of  $R_p$  (Table 3), decreases with rising pH. The corrosion rate values obtained using both methods are in good agreement.

In a neutral environment, the formation of a passive layer on the steel surface significantly reduces the occurrence of corrosion reactions, allowing the steel to behave similarly to stainless steel.

### 3.4 Appearance of the sample surfaces before and after electrochemical testing

Figure 4 shows the surface of the steel sample before electrochemical tests (a) and after testing in acidic (b) and neutral (c) solutions.



**Figure 4** Sample surfaces a) before electrochemical tests, b) after electrochemical testing in pH 2.9 solution, c) after electrochemical testing in pH 6.5 solution

Before electrochemical testing (Figure 4a), no traces of corrosion or other damage are visible on the sample's surface, as proper sample preparation was ensured. In the acidic NaCl solution, intensive dissolution of the metal surface occurs in the anodic region, resulting in visible traces of dissolution on the sample surface (Figure 4b). In the neutral NaCl solution, the steel surface remains passive, and dissolution occurs at an extremely low rate only through the pores in the passive film, leaving the surface largely unaffected (Figure 4c).

#### 4 CONCLUSION

The polarization resistance ( $R_p$ ), corrosion current density ( $j_{\text{corr}}$ ), and corrosion rate ( $v_{\text{corr}}$ ) were used as indicators of the resistance to general (uniform) corrosion. As the pH value of the NaCl solutions increased, the tested steel exhibited higher corrosion resistance.

In the acidic NaCl solution, the steel did not enter a passive state and dissolved rapidly. In contrast, in the neutral NaCl solution, a passive layer formed on the steel surface, protecting it from further corrosion.

The corrosion rate results obtained using linear polarization resistance (LPR) and electrochemical impedance spectroscopy (EIS) methods are in good agreement, confirming the consistency of the electrochemical techniques employed.

#### ACKNOWLEDGEMENTS

This work was financially supported by the Ministry of Science, Technological Development and Innovation of the Republic of Serbia and the Ministry of Higher Education, Science and Innovation of the Republic of Slovenia, under the joint Serbia-Slovenia project for the period 2023-2025.

**REFERENCES**

ASTM A335 (2022) Standard Specification for Seamless Ferritic Alloy-Steel Pipe for High-Temperature Service.

BENDICK, W. and RING, M. (1996) Creep rupture strength of tungsten-alloyed 9-12 % Cr steels for piping in power plants. *Steel Research*, 67, pp. 382-385.

GARR, K., RHODES, C., and KRAMER, D. (1973) Effects of Microstructure on Swelling and Tensile Properties of Neutron-Irradiated Types 316 and 405 Stainless Steels, *ASTM Selected Technical Papers*, pp. 109-121.

HAARMANN, K. et al. (2002) *The T91/P91 Book*. Boulogne: Vallourec and Mannesmann Tubes.

HIRSCHORN, B., ORAZEM, M.E., TRIBOLLET, B., VIVIER, V., FRATEUR, I., and MUSIANI, M. (2010) Constant-phase element behavior caused by resistivity distributions in films: II. Applications. *Journal of The Electrochemical Society*, 157, C458.

LITTLE, E.A. (1972) Voids produced in mild steel by 1MeV electron irradiation. *Radiation Effects*, 16, pp. 135-137.

SRINIVASAN, R. and FASMIN, F. (2021) *An introduction to electrochemical impedance spectroscopy*. Boca Raton: CRC Press.